ANTICANCER RESEARCH *37*: 455-464 (2017)
doi:10.21873/anticanres.11337

Fumonisin B1 Inhibits Endoplasmic Reticulum Stress Associated-apoptosis After FoscanPDT Combined with C6-Pyridinium Ceramide or Fenretinide

NITHIN B. BOPPANA[1], JACQUELINE M. KRAVEKA[2], MEHRDAD RAHMANIYAN[2], LI LI[2], ALICJA BIELAWSKA[3], JACEK BIELAWSKI[3], JASON S. PIERCE[3], JEREMY S. DELOR[1], KEZHONG ZHANG[4], MLADEN KORBELIK[5] and DUSKA SEPAROVIC[1,6]

[1]*Department of Pharmaceutical Sciences, Eugene Applebaum College of Pharmacy and Health Sciences, and* [6]*Karmanos Cancer Institute, Wayne State University, Detroit, MI, U.S.A.;*
[2]*Department of Pediatrics Division of Hematology-Oncology, Charles Darby Children's Research Institute, and Hollings Cancer Center, Medical University of South Carolina, Charleston, SC, U.S.A.;*
[3]*Department of Biochemistry and Molecular Biology, Medical University of South Carolina, Charleston, SC, U.S.A.;*
[4]*Center for Molecular Medicine and Genetics and Department of Immunology and Microbiology, Wayne State University School of Medicine, Wayne State University, Detroit, MI, U.S.A.;*
[5]*British Columbia Cancer Agency, Vancouver, BC, Canada*

Abstract. *Background/Aim: Combining an anticancer agent fenretinide (HPR) or C6-pyridinium ceramide (LCL29) with Foscan-mediated photodynamic therapy (FoscanPDT) is expected to augment anticancer benefits of each substance. We showed that treatment with FoscanPDT+HPR enhanced accumulation of C16-dihydroceramide, and that fumonisin B1 (FB), an inhibitor of ceramide synthase, counteracted caspase-3 activation and colony-forming ability of head and neck squamous cell carcinoma (HNSCC) cells. Because cancer cells appear to be more susceptible to increased levels of the endoplasmic reticulum (ER) stress than normal cells, herein we tested the hypothesis that FoscanPDT combined with HPR or LCL29 induces FB-sensitive ER stress-associated apoptosis that affects cell survival. Materials and Methods: Using an HNSCC cell line, we determined: cell survival by clonogenic assay, caspase-3 activity by spectrofluorometry, the expression of the ER markers BiP and CHOP by quantitative real-time polymerase chain reaction and western immunoblotting, and sphingolipid levels by mass spectrometry. Results: Similar to HPR+FoscanPDT, LCL29+FoscanPDT induced enhanced loss of clonogenicity and caspase-3 activation, that were both inhibited by FB. Our additional pharmacological evidence showed that the enhanced loss of clonogenicity after the combined treatments was singlet oxygen-, ER stress- and apoptosis-dependent. The combined treatments induced enhanced, FB-sensitive, up-regulation of BiP and CHOP, as well as enhanced accumulation of sphingolipids. Conclusion: Our data suggest that enhanced clonogenic cell killing after the combined treatments is dependent on oxidative- and ER-stress, apoptosis, and FB-sensitive sphingolipid production, and should help develop more effective mechanism-based therapeutic strategies.*

Correspondence to: Dr. Duska Separovic, Department of Pharmaceutical Sciences, Eugene Applebaum College of Pharmacy and Health Sciences, Wayne State University, 259 Mack Ave., Detroit, MI 48201, U.S.A. Tel: +13135778065, Fax: +13135772033, e-mail: jmjilyss999@gmail.com

Key Words: Apoptosis, ER stress, fenretinide, fumonisin, LCL29, PDT, sphingolipids.

Although FoscanPDT alone was effective in treating early HNSCC, it was not as successful for recurrent HNSCC (1). Thus, there is a need to combine PDT with other anticancer agents for the purpose of achieving synergism of the anticancer benefits of each, with minimal toxicity. A good candidate for the combined treatment with FoscanPDT is HPR, an FDA-approved anticancer treatment, with minimal toxicity to normal cells (2, 3). We showed that in SCCVII squamous cell carcinoma tumors grown in syngeneic mice, FoscanPDT+HPR improved the therapeutic outcome (4). Using the same *in vivo* model we showed that combining FoscanPDT with LCL29, significantly enhanced tumor cures (5, 6). These agents affect the levels of sphingolipids, which can also act as anticancer agents. We and others showed that

the *de novo* sphingolipid biosynthesis pathway is associated with apoptosis after exposure to stressors, including PDT and HPR, in HNSCC cells (7-11). The *de novo* sphingolipid biosynthesis pathway includes a ceramide synthase-dependent conversion of dihydrosphingosine to dihydroceramide, which is then converted, in a desaturase-dependent reaction, to ceramide (Figure 1). Desaturase 1, the ubiquitous isoform of desaturase, is inhibited by HPR (12). Dihydroceramide can be catabolized to dihydrosphingosine *via* ceramidase (13), and dihydrosphingosine can be phosphorylated by sphingosine kinase to dihydrosphingosine-1-phosphate (14). We showed that treatment of HNSCC cells with FoscanPDT+HPR enhanced accumulation of C16-dihydroceramide and caspase-3 activation (4). The ceramide synthase inhibitor FB (15) significantly reduced caspase-3 activation and the colony-forming ability of HNSCC cells after FoscanPDT±HPR (4).

Both FoscanPDT and HPR can induce cancer cell death *via* ER stress (16, 17). Cancer cells appear to be more susceptible to increased levels of ER stress than their normal counterparts (18). ER stress, triggered by stress and an imbalance between the load of unfolded or misfolded proteins inside the ER lumen and the capacity of the ER, results in the unfolded protein response, *i.e.* the build up of unfolded or misfolded proteins in the ER (19). The unfolded protein response involves the induction of three signaling pathways: the double-stranded RNA-activated protein kinase-like ER kinase (PERK)-eukaryotic translation initiation factor 2 alpha (eIF2α), activating transcription factor 6 (ATF6), and the inositol-requiring enzyme 1 (IRE1)-X-box binding protein 1 (XBP1) (20). These signaling pathways counteract stress by inducing the expression of ER chaperones, binding immunoglobulin protein (BiP), and other factors, that together promote the protein folding machinery (21). If the unfolded protein response fails to control the levels of unfolded and misfolded proteins in the ER, ER-induced apoptosis is triggered through activation of the pro-apoptotic factor CCAAT/enhancer-binding protein homologous protein (CHOP) (22).

In HNSCC cells the ER stress-mediated apoptosis involves the *de novo* sphingolipid biosynthesis pathway-associated ceramide synthase (11). It is not known, however, whether the ER stress-associated apoptosis is induced after combining FoscanPDT with HPR or LCL29, and whether sphingolipids modulate the pathway. In the present study we tested the hypothesis that FoscanPDT combined with HPR or LCL29 induces FB-sensitive ER stress-associated apoptosis that affects cell survival.

Materials and Methods

Materials. The photosensitizer Foscan (m-tetrahydroxyphenylchlorin, Biolitec AG, Edinburgh, UK) was dissolved (2 mg/ml) in a mixture of ethanol:polyethyleneglycol200:water (2/3/5, v/v). C6-pyridinium ceramide or LCL29 [D-erythro-2-N-[6'-1"-pyridinium-hexanoyl sphingosine bromide] was obtained from Avanti Polar Lipids (Alabaster, AL, USA). DMEM/F-12 medium was obtained from Thermo-Fisher Scientific (Waltham, MA, USA). Fetal bovine serum, HPR [N-(4-hydroxyphenyl) retinamide], L-histidine, and 4-phenylbutyrate were all purchased from Sigma-Aldrich (St. Louis, MO, USA). Fumonisin B1 and zVAD-fmk were from Cayman Chemicals (Ann Arbor, MI, USA) and MBL International Corporation (Woburn, MA, USA), respectively. 4-mu8c, salubrinal and thapsigargin were all obtained from EMD Millipore (Billerica, MA, USA).

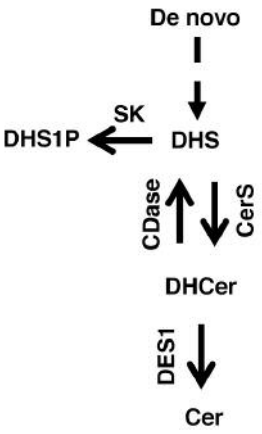

Figure 1. *De novo sphingolipid biosynthesis pathway-associated metabolism of dihydrosphingolipids. CDase, Ceramidase; Cer, ceramide; CerS, ceramide synthase; DES1, desaturase 1; DHCer, dihydroceramide; DHS, dihydrosphingosine; DHS1P, dihydrosphingosine-1-phosphate; SK, sphingosine kinase.*

Cell culture and treatments. SCC19 cells were kindly provided by Dr. Thomas Carey (University of Michigan, Ann Arbor, MI, USA). Cells were grown in DMEM/F-12 medium containing 10% fetal bovine serum, 100 units/ml penicillin, and 100 μg/ml streptomycin (Life Technologies, Carlsbad, CA, USA) in a humidified incubator at 37˚C and 5% CO_2. For all experiments, incubation of cells was carried out in a humidified incubator at 37˚C and 5% CO_2. All treatments were added to the cells in the growth medium. After overnight incubation with Foscan, LCL29 (1 μM) or HPR (2.5 μM) were added immediately prior to irradiation. Cells were irradiated at room temperature with red light (power density: 2 mW/cm^2; fluence: 400 mJ/cm^2; λ_{max} ~ 670 nm), using a light-emitting diode array light source (EFOS, Mississauga, ON, Canada), and incubated for the indicated times. The inhibitors were used at their non-toxic doses (LD <5) and were added 1 h prior to individual or combined treatments. FoscanPDT, LCL29 and HPR were used at their LD20s. With the exception of the clonogenic assay, in all other assays used in the present study, the total number of cells exposed to the treatments was in the range of 1-2×10^6. In the clonogenic assays using preplating and postplating protocols, the total number of cells was approximately 500 and 1×10^6, respectively. At the constant fluence of 400 mJ/cm^2, the final concertation of Foscan of 0.06 μM and 0.15 μM in preplating and postplating protocols, respectively, was required to result in the LD20. Apparently, there was a correlation between the total number of cells exposed to FoscanPDT and the actual LD20. This was not the case for LCL29 or HPR alone.

Clonogenic assay. Cell survival was assessed using clonogenic assay according to the preplating and postplating protocols (23, 24). For the preplating protocol, cells were resuspended in the growth medium containing Foscan (0.06 μM) and aliquots were seeded in 6-well plates (Thermo-Fisher Scientific) in triplicate in sufficient numbers to give rise to approximately 50 colonies per well. After overnight incubation, cells were irradiated. Other treatments and inhibitors were added prior to irradiation, as described above. For the postplating protocol, cells were grown in T25 flasks (Thermo-Fisher Scientific) and treated with FoscanPDT (0.15 μM Foscan + 400 mJ/cm^2)±LCL29 or HPR. Overnight incubation with Foscan was followed by addition of other treatments and irradiation. After treatments, cells were trypsinized and aliquots were plated in triplicate in sufficient numbers to give rise to approximately 50 colonies per well. For both protocols, after 10 days of incubation, colonies were stained with crystal violet (0.1%) and counted. Plating efficiency was 28% (n=42).

DEVDase (caspase-3) activity assay. As described previously (8), DEVDase activity was determined in the cytosol obtained from treated cells by an assay based on the enzyme's cleavage of a fluorogenic derivative of the tetrapeptide substrate N-acetyl-Asp-Glu-Val-Asp (DEVD; Enzo Life Sciences, Farmingdale, NY, USA). The fluorescence of the cleaved DEVD substrate was measured using a spectrofluorometer (F-2500 Hitachi, New York, NY, USA; 380 nm excitation, 460 nm emission).

RNA extraction and quantitative real-time polymerase chain reaction (RT-PCR). Total RNA was isolated from treated cells using RNeasy® Mini Kit (Qiagen, Valencia, CA, USA) according to manufacturer's instructions. cDNA was synthesized from 1 μg of the total RNA using iScript™ cDNA Synthesis Kit (Bio-Rad, Hercules, CA, USA). The concentration and quality of total RNA preparations were evaluated spectrophotometrically. RT-PCR was performed on a Bio-Rad CFX96 detection system using Bio-Rad SsoFast Probes Supermix™ and TaqMan® Gene Expression Assays (Life Technologies) with primer/probe sets for CHOP and BiP, the ribosomal protein L13A, and hypoxanthine-guanine phosphoribosyltransferase (all from Life Technologies). Initial steps of RT-PCR were 30 s at 85˚C, followed by 40 cycles consisting of a 5 sec at 95˚C, followed by 10 sec at 60˚C. Determination of the relative normalized expression of corresponding CHOP and BiP mRNAs against the internal control housekeeping genes, the ribosomal protein L13A and hypoxanthine-guanine phosphoribosyltransferase was performed by ΔΔCT provided by CFX96 manager software 3.0 from Bio-Rad.

Immunoblotting. After treatments, cells were collected, lysed in reducing Laemmli buffer, boiled and then subjected to sodium dodecyl sulfate polyacrylamide gel electrophoresis (SDS-PAGE), and western immunoblotting (25). Equal protein loading was confirmed using antibody to actin. Antibodies to BiP, CHOP and actin were from Enzo-Life Sciences, Thermo-Fisher Scientific, and EMD Millipore, respectively. Following visualization of blots using ECL Plus chemifluorescence kit and STORM 860 imaging system (GE Healthcare, Piscataway, NJ, USA), they were quantified by ImageQuant 5.2 (GE Healthcare).

Electrospray ionization tandem mass spectrometry (MS) analysis. Lipids were extracted from treated cells, and sphingolipids were separated by high performance liquid chromatography, introduced to electrospray ionization source and then analyzed by tandem MS using Thermo Scientific Vanquish Ultra-High Performance Liquid Chromatography System and Thermo Scientific TSQ Quantum Access Max Triple Quadrupole Mass Spectrometer (both from Thermo-Fisher Scientific) [cf. (25)].

Protein determination. Protein content was determined by a modified Bradford assay (Bio-Rad).

Statistical analysis. Significant differences ($p<0.05$) were determined using Student's *t*-test.

Results and Discussion

Enhanced loss of clonogenicity after the combined treatments is dependent on oxidative- and ER- stress, apoptosis, and FB-sensitive sphingolipid production. To assess the role of oxidative and ER stress, apoptosis and FB-sensitive sphingolipid generation in cell survival after FoscanPDT combined with HPR or LCL29, we used the following pharmacologic inhibitors: the singlet oxygen quencher L-histidine (27), the ceramide synthase inhibitor FB, the pan-caspase inhibitor zVAD-fmk (28), and the ER stress-related agents. As shown in Figure 2, enhanced loss of clonogenicity was induced after FoscanPDT combined with LCL29 or HPR, and the effect was counteracted by L-histidine, FB and zVAD-fmk. The ER stress inducer thapsigargin (29) augmented enhanced loss of clonogenicity after FoscanPDT+HPR. Enhanced loss of clonogenicity after the combined treatments was counteracted by: 4-mu8c, an inhibitor of IRE1 (30), salubrinal, an inhibitor of dephosphorylation of eIF2α (31), and 4-phenylbutyrate, an inhibitor of CHOP (32). The data suggest that the combined treatments induced enhanced loss of clonogenicity that were dependent upon singlet oxygen, ER stress, apoptosis and FB-sensitive sphingolipid generation.

FB inhibited caspase-3 activation after FoscanPDT alone or in combination with LCL29. We showed that after FoscanPDT+HPR caspase-3 activation was enhanced. FB counteracted caspase-3 activation after FoscanPDT±HPR (4). Similarly, enhanced caspase-3 activation was induced after FoscanPDT+LCL29, and inhibited by FB (Figure 3). The data suggest that enhanced caspase-3 activation after FoscanPDT+LCL29 is dependent upon FB-sensitive sphingolipid generation.

The effect of FoscanPDT±LCL29±FB on BiP and CHOP mRNA expression. To assess the induction of ER stress after treatments, we determined the expression of the ER stress markers BiP and CHOP. As shown in Figure 4A, the ER stress prosurvival marker *BiP* was up-regulated at the mRNA level after FoscanPDT alone. BiP mRNA was down-regulated after LCL29 alone, and the effect was counteracted

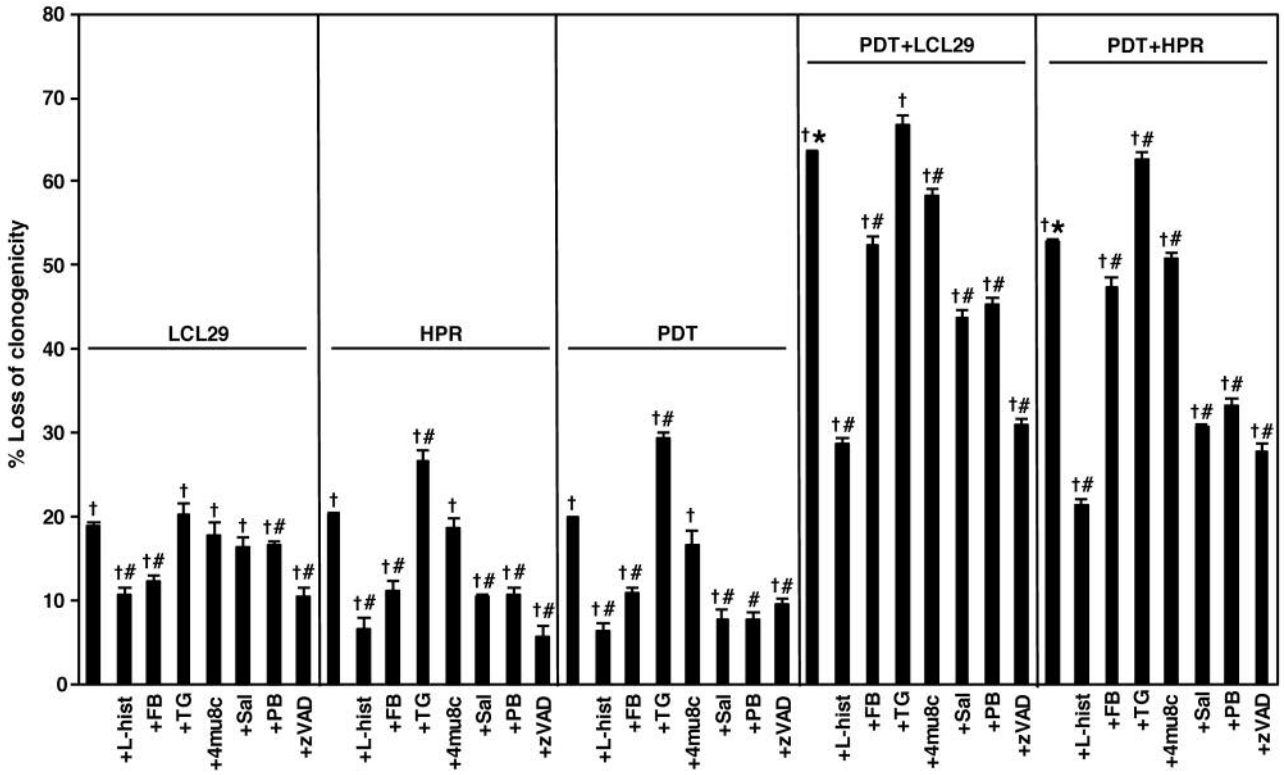

Figure 2. *Enhanced loss of clonogenicity after combined treatments is dependent on oxidative- and ER-stress, apoptosis, and FB-sensitive sphingolipid production. L-histidine (L-hist; 1 mM), fumonisin B1 (FB; 10 μM), thapsigargin TG (1 nM), 4-mu8c (1 μM), salubrinal (Sal; 5 μM), 4-phenylbutyrate (PB; 2 mM), and zVAD-fmk (zVAD; 10 μM) were added 1 h prior to FoscanPDT (0.06 μM Foscan + 400 mJ/cm^2), LCL29 (1 μM), HPR (2.5 μM) or the combined treatments. Colonies were stained with crystal violet (0.1%) and counted 10 days after treatments. The data are shown as the average±SEM (n=3-39). Significant differences are shown between: †treatment and untreated control; *combination and individual treatments; #(treatment+inhibitor) and treatment. Untreated controls had 0% loss of clonogenicity.*

after combining LCL29 with FoscanPDT. FB had no significant effect on BiP mRNA after FoscanPDT±LCL29. The ER stress proapoptotic marker CHOP mRNA was up-regulated after FoscanPDT±LCL29 (Figure 4A). FB modesty (but insignificantly) attenuated enhanced *CHOP* mRNA expression after FoscanPDT+LCL29, and had no significant effect on *CHOP* mRNA levels after each treatment alone.

The effect of FoscanPDT±HPR±FB on BiP and CHOP mRNA expression. In contrast to FoscanPDT alone, there was no up-regulation of *BiP* mRNA after HPR alone (Figure 4B). FB had no significant effect on BiP mRNA levels after FoscanPDT or HPR alone. Enhanced up-regulation of *BiP* mRNA after FoscanPDT+HPR was inhibited by FB. *CHOP* mRNA levels were elevated after individual treatments and were unaffected by FB. Enhanced *CHOP* mRNA expression after FoscanPDT+HPR was attenuated by FB.

The effect of treatments on CHOP and BiP protein expression. As depicted in Figure 4C, elevated CHOP protein expression was induced after FoscanPDT alone or in combination with LCL29 or HPR. LCL29 or HPR alone did not induce CHOP protein expression. FB inhibited induced CHOP protein expression after FoscanPDT alone or in combination with LCL29 or HPR. BiP was up-regulated at the protein level only after the combinations, and FB attenuated the effect. Overall, the combined treatments induced enhanced BiP and CHOP expression that was inhibited by FB at the mRNA and/or protein level. The data imply that FB-sensitive sphingolipid generation modulates enhanced up-regulation of BiP and CHOP after the combined treatments. Our findings also indicate that the long-term effect of enhanced expression of the prosurvival BiP and the proapoptotic CHOP was tipping the balance in favor of enhanced loss of clonogenicity.

Enhanced accumulation of sphingolipids is induced after treatments. We showed that treatment with FoscanPDT+HPR enhanced accumulation of C16-dihydroceramide (4). Similar trend was shown only for C18:1-ceramide, not for any other

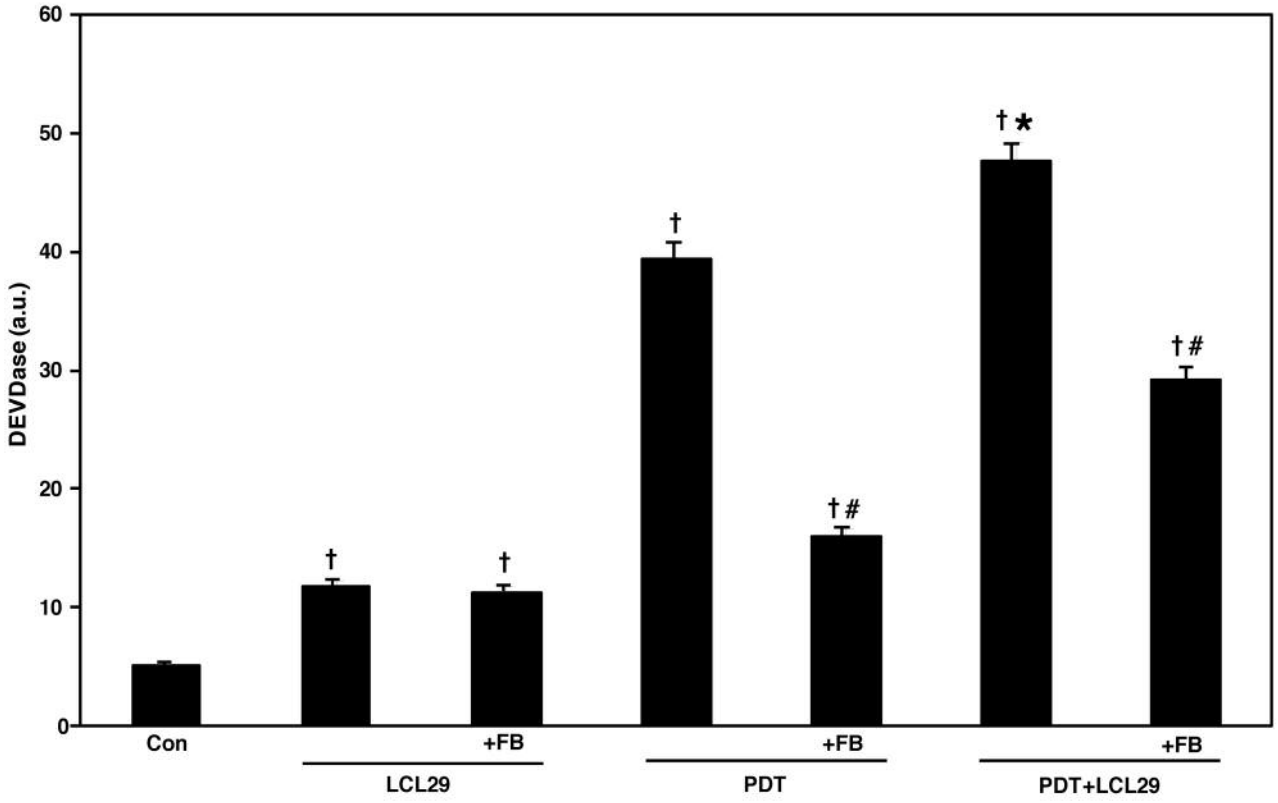

Figure 3. *Enhanced caspase-3 activation after FoscanPDT+LCL29 is inhibited by FB. FB (10 μM) was added 1 h prior to PDT (0.15 μM Foscan + 400 mJ/cm^2), LCL29 (1 μM) or the combination. Twenty-four hours after treatments, cells were collected and processed for DEVDase assay. The enzyme activity is expressed in arbitrary units (a.u.) and the data are shown as the average±SEM (n=2-6). Significant differences are shown between: †treatment and untreated control (Con); *combination and individual treatments; #(treatment+FB) and treatment.*

ceramide (4). Here we show that combining FoscanPDT with HPR enhanced accumulation of dihydrosphingosine-1-phosphate (Table I). Moreover, the combination of FoscanPDT with LCL29 enhanced accumulation of the dihydrosphingolipids C16-dihydroceramide, dihydrosphingosine, and dihydrosphingosine-1-phosphate, as well as C18-ceramide (Figure 5). Similar trends were observed for other ceramides, *i.e.* C14-, C16-, and C26:1-ceramide, as well as sphingosine-1-phosphate (Table II).

Taken together, the combined treatments enhanced the levels of dihydrosphingolipids and enhanced the ER stress and apoptosis. Because dihydroceramide can be converted into dihydrosphingosine and dihydrosphingosine-1-phosphate, this can lead to cell death or survival depending on dihydrosphingosine/dihydrosphingosine-1-phosphate balance (13). Similar reasoning could be applied to increases in the proapoptotic ceramide and the prosurvival sphingosine-1-phosphate after FoscanPDT+LCL29. The enhanced loss of clonogenicity after the combined treatments indicates that the dihydrosphingosine/dihydrosphingosine-1-phosphate and ceramide/sphingosine-1-phosphate balances were tipped in favor of this outcome.

In summary, our present study indicates that enhanced loss of clonogenicity after the combined treatments is dependent on oxidative- and ER- stress, apoptosis, and FB-sensitive sphingolipid production. The study also provides novel insights into modulation of the ER stress by FB-sensitive sphingolipid production after the combined treatments. These novel findings are expected to help develop more effective mechanism-based therapeutic strategies.

Acknowledgements

This work was supported by: the Faculty Research Award Program Individual Investigator Award from the Eugene Applebaum College of Pharmacy and Health Sciences, Wayne State University, Detroit, MI, USA (to DS). The MS-related work at the Lipidomics Shared Resource Facility (Medical University of South Carolina, Charleston, SC, USA) was supported by the following grants from the National Institutes of Health (NIH): P30 CA 138313, SC COBRE P20 RR017677, and C06 RR018823.

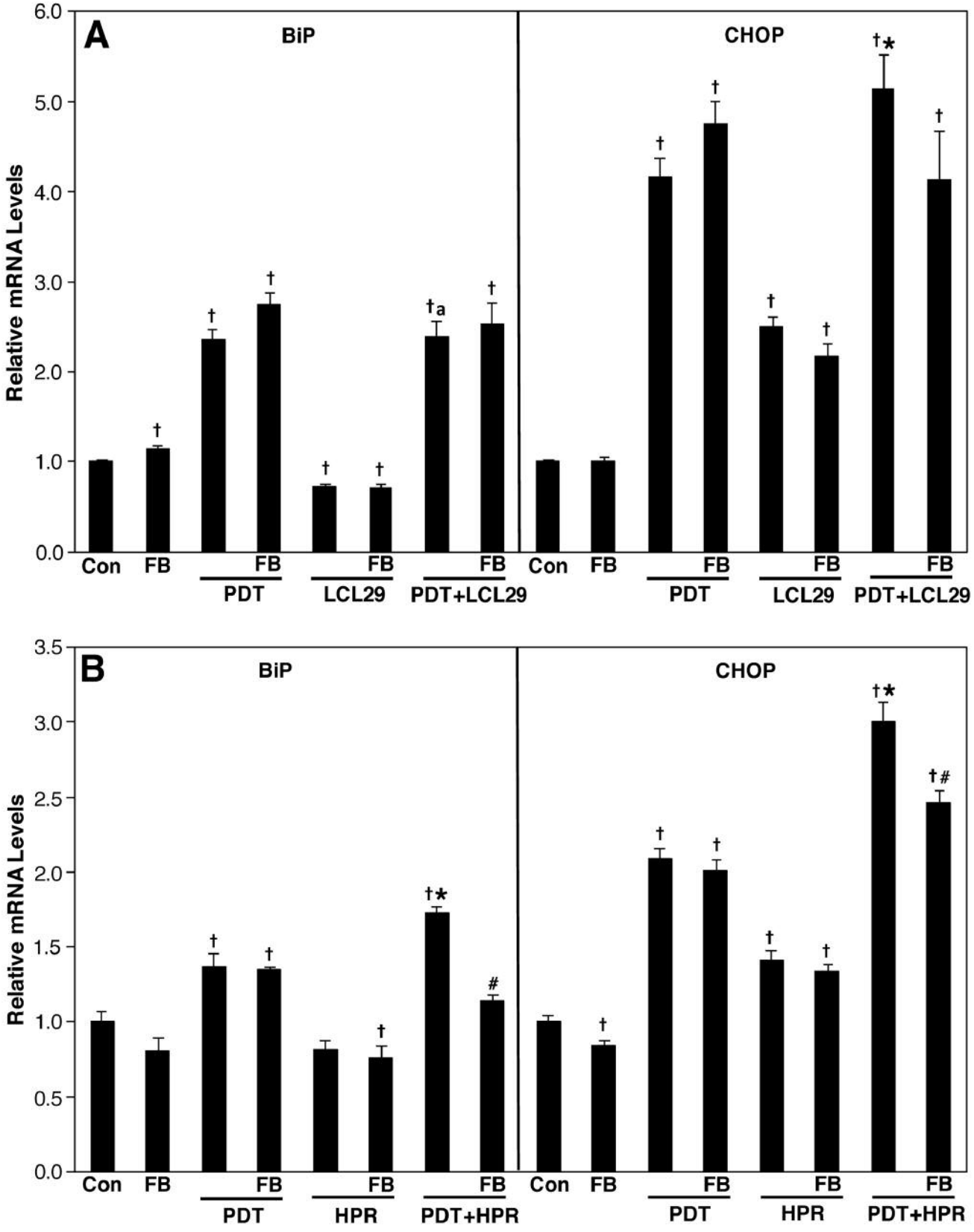

Figure 4. *Continued*

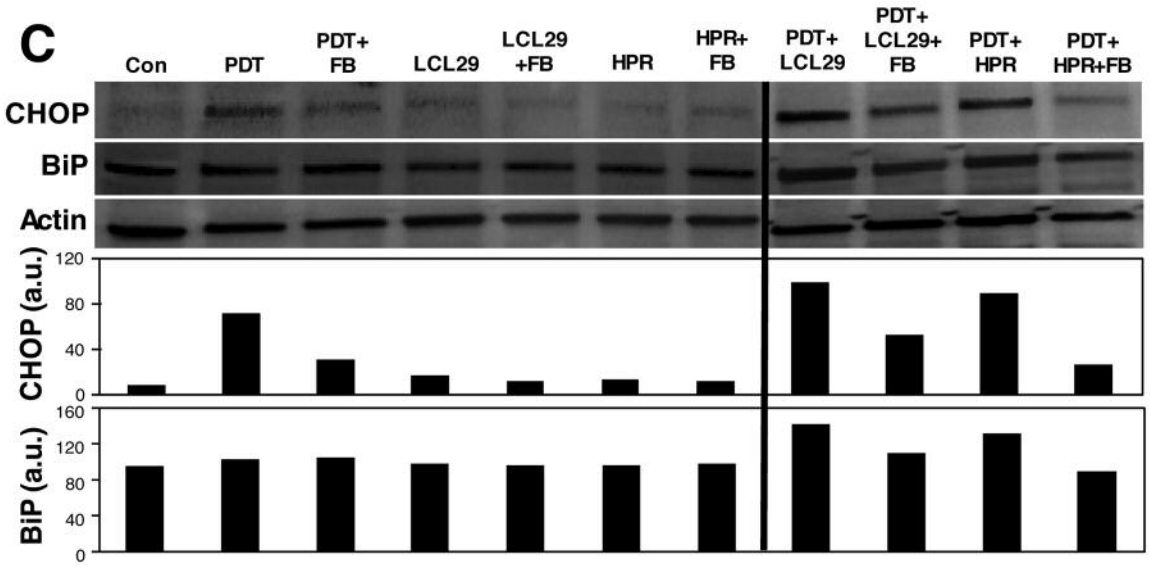

Figure 4. *The effect of treatments without and with FB on BiP and CHOP expression. FB (10 μM) was added 1 h prior to PDT (0.15 μM Foscan + 400 mJ/cm^2), LCL29 (1 μM), HPR (2.5 μM) or the combinations. After the treatments, the cells were incubated for the indicated times, collected, and processed for appropriate assays. (A and B): The effect of treatments±FB on BiP and CHOP mRNA levels. Twenty-four hours after the treatments, the cells were collected and processed for RT-PCR. The data were calculated as the relative normalized expression of BiP and CHOP mRNAs against the expression of housekeeping gene-encoding proteins the ribosomal protein L13A and hypoxanthine-guanine phosphoribosyltransferase, and are shown as the average±SEM (n=2-4). Significant differences are shown between: †treatment and untreated control (Con); *combination and individual treatments; #(treatment+FB) and treatment; acombination and LCL29. (C): The effect of treatments±FB on BiP and CHOP protein levels. Forty eight hours post-treatments, cells were collected and processed for PAGE/western immunoblotting. Equal protein loading was verified using anti-actin. Protein levels were quantified from the blots and are expressed in arbitrary units (a.u.).*

References

1 Biel MA: Photodynamic therapy of head and neck cancers. Methods Mol Biol *635*: 281-293, 2010.

2 Bonanni B, Lazzeroni M and Veronesi U: Synthetic retinoid fenretinide in breast cancer chemoprevention. Expert Rev Anticancer Ther *7*: 423-432, 2007.

3 Maurer BJ, Kang MH, Villablanca JG, Janeba J, Groshen S, Matthay KK, Sondel PM, Maris JM, Jackson HA, Goodarzian F, Shimada H, Czarnecki S, Hasenauer B, Reynolds CP and Marachelian A: Phase I trial of fenretinide delivered orally in a novel organized lipid complex in patients with relapsed/refractory neuroblastoma: a report from the New Approaches to Neuroblastoma Therapy (NANT) consortium. Pediatr Blood Cancer *60*: 1801-1808, 2013.

4 Boppana NB, DeLor JS, Van Buren E, Bielawska A, Bielawski J, Pierce JS, Korbelik M and Separovic D: Enhanced apoptotic cancer cell killing after Foscan photodynamic therapy combined with fenretinide *via de novo* sphingolipid biosynthesis pathway. J Photochem Photobiol B *159*: 191-195, 2016.

5 Separovic D, Bielawski J, Pierce JS, Merchant S, Tarca AL, Bhatti G, Ogretmen B and Korbelik M: Enhanced tumor cures after Foscan photodynamic therapy combined with the ceramide analog LCL29. Evidence from mouse squamous cell carcinomas for sphingolipids as biomarkers of treatment response. Int J Oncol *38*: 521-527, 2011.

6 Breen P, Joseph N, Thompson K, Kraveka JM, Gudz TI, Li L, Rahmaniyan M, Bielawski J, Pierce JS, Van Buren E, Bhatti G and Separovic D: Dihydroceramide desaturase knockdown impacts sphingolipids and apoptosis after photodamage in human head and neck squamous carcinoma cells. Anticancer Res *33*: 77-84, 2013.

7 Separovic D, Breen P, Joseph N, Bielawski J, Pierce JS, Van Buren E and Gudz TI: Ceramide synthase 6 knockdown suppresses apoptosis after photodynamic therapy in human head and neck squamous carcinoma cells. Anticancer Res *32*: 753-760, 2012.

8 Separovic D, Breen P, Joseph N, Bielawski J, Pierce JS, Van Buren E and Gudz TI: siRNA-mediated down-regulation of ceramide synthase 1 leads to apoptotic resistance in human head and neck squamous carcinoma cells after photodynamic therapy. Anticancer Res *32*: 2479-2485, 2012.

Table I. *FoscanPDT+HPR enhances accumulation of dihydrosphingosine-1-phosphate in SCC19 cells at 24 h.*

	Con	HPR	PDT	PDT+HPR
DHS1P	0.7±0.3	4.4±0.2	15.0±1.7	92.8±12.8

SCC19 cells were treated with PDT (0.15 μM Foscan + 400 mJ/cm^2)±HPR (2.5 μM), incubated for 24 h, collected, and processed for MS. Sphingolipid levels were calculated as pmoles/mg protein and are shown as the average±SEM (n=2-3). Con, untreated control; DHS1P, dihydrosphingosine-1-phosphate.

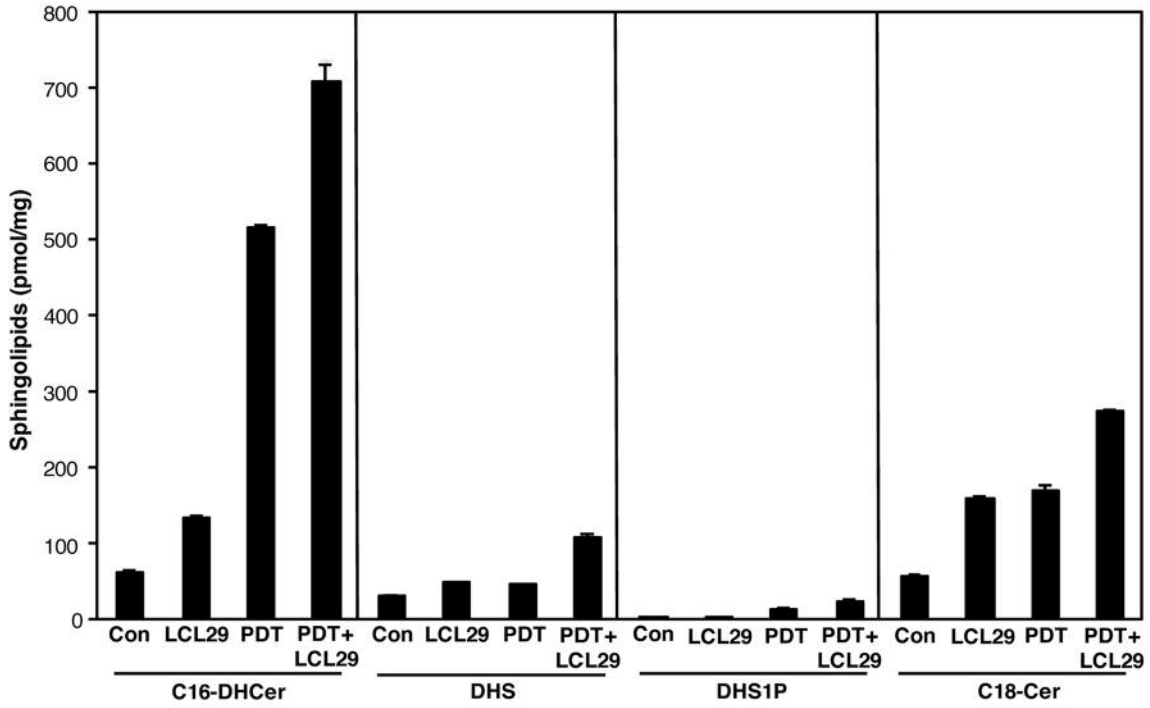

Figure 5. *FoscanPDT+LCL29 induces enhanced accumulation of dihydrosphingolipids and C18-ceramide. Cells were treated with PDT (0.15 μM Foscan + 400 mJ/cm^2)±LCL29 (1 μM), incubated for 24 h, then collected and processed for MS. The levels of sphingolipids were calculated as pmoles/mg protein and are shown as the average±SEM (n=2-3). C16-DHCer, C16-dihydroceramide; DHS, dihydrosphingosine; DHS1P, dihydrosphingosine-1-phosphate; C18-Cer, C18-ceramide.*

Table II. *Effect of FoscanPDT±LCL29 on sphingolipid levels in SCC19 cells at 24 h.*

	Con	LCL29	PDT	PDT+LCL29
C14-Cer	7.1±0.2	19.6±1.6	18.3±0.7	27.0±0.1
C16-Cer	134.4±6.7	312.2±14.7	245.3±13.7	345.1±6.5
C18-Cer	57.2±3.2	160.6±2.6	171.2±7.8	274.7±2.2
C18:1-Cer	6.0±0.2	25.1±0.8	24.0±4.5	23.9±1.3
C20-Cer	31.1±3.4	80.3±1.6	59.2±3.2	87.0±1.4
C20:1-Cer	5.4±0.1	18.4±1.2	15.7±1.0	21.3±0.8
C22-Cer	63.2±0.2	96.9±5.0	70.2±3.2	82.6±1.7
C22:1-Cer	27.6±2.9	69.8±2.1	47.0±0.8	62.4±1.3
C24-Cer	390.2±26.9	297.3±26.7	217.5±12.0	249.0±3.4
C24:1-Cer	342.4±7.5	591.7±10.2	462.6±15.5	552.9±25.5
C26-Cer	37.8±0.8	24.1±1.6	27.3±1.6	34.4±2.0
C26:1-Cer	46.8±2.5	46.4±3.8	79.6±2.4	89.3±3.4
S1P	0.7±0.1	3.3±0.4	1.5±0.4	4.5±0.1

SCC19 cells were treated with PDT (0.15 μM Foscan + 400 mJ/cm^2) ±LCL29 (1 μM), incubated for 24 h, collected, and processed for MS. Sphingolipid levels were calculated as pmoles/mg protein and are shown as the average±SEM (n=2-3). Con, Untreated control; Cer, ceramide; S1P, sphingosine-1-phosphate.

9 Senkal CE, Ponnusamy S, Bielawski J, Hannun YA and Ogretmen B: Antiapoptotic roles of ceramide-synthase-6-generated C16-ceramide *via* selective regulation of the ATF6/CHOP arm of ER-stress-response pathways. Faseb J *24*: 296-308, 2010.

10 Senkal CE, Ponnusamy S, Manevich Y, Meyers-Needham M, Saddoughi SA, Mukhopadyay A, Dent P, Bielawski J and Ogretmen B: Alteration of Ceramide Synthase 6/C16-Ceramide Induces Activating Transcription Factor 6-mediated Endoplasmic Reticulum (ER) Stress and Apoptosis *via* Perturbation of Cellular Ca^{2+} and ER/Golgi Membrane Network. J Biol Chem *286*: 42446-42458, 2011.

11 Kraveka JM, Li L, Szulc ZM, Bielawski J, Ogretmen B, Hannun YA, Obeid LM and Bielawska A: Involvement of dihydroceramide desaturase in cell cycle progression in human neuroblastoma cells. J Biol Chem *282*: 16718-16728, 2007.

12 Fabrias G, Munoz-Olaya J, Cingolani F, Signorelli P, Casas J, Gagliostro V and Ghidoni R: Dihydroceramide desaturase and dihydrosphingolipids: debutant players in the sphingolipid arena. Prog Lipid Res *51*: 82-94, 2012.

13 Berdyshev EV, Gorshkova IA, Usatyuk P, Zhao Y, Saatian B, Hubbard W and Natarajan V: *De novo* biosynthesis of dihydrosphingosine-1-phosphate by sphingosine kinase 1 in mammalian cells. Cell Signal *18*: 1779-1792, 2006.

14 Wang E, Norred WP, Bacon CW, Riley RT and Merrill AH Jr.: Inhibition of sphingolipid biosynthesis by fumonisins. Implications for diseases associated with Fusarium moniliforme. J Biol Chem *266*: 14486-14490., 1991.

15 Armstrong JL, Flockhart R, Veal GJ, Lovat PE and Redfern CP: Regulation of endoplasmic reticulum stress-induced cell death

by ATF4 in neuroectodermal tumor cells. J Biol Chem *285*: 6091-6100, 2010.
16 Marchal S, Francois A, Dumas D, Guillemin F and Bezdetnaya L: Relationship between subcellular localisation of Foscan and caspase activation in photosensitised MCF-7 cells. Br J Cancer *96*: 944-951, 2007.
17 Schonthal AH: Endoplasmic reticulum stress and autophagy as targets for cancer therapy. Cancer Lett *275*: 163-169, 2009.
18 Ron D and Walter P: Signal integration in the endoplasmic reticulum unfolded protein response. Nat Rev Mol Cell Biol *8*: 519-529, 2007.
19 Sano R and Reed JC: ER stress-induced cell death mechanisms. Biochim Biophys Acta *1833*: 3460-3470, 2013.
20 Zhu G and Lee AS: Role of the unfolded protein response, GRP78 and GRP94 in organ homeostasis. J Cell Physiol *230*: 1413-1420, 2015.
21 Yamaguchi H and Wang HG: CHOP is involved in endoplasmic reticulum stress-induced apoptosis by enhancing DR5 expression in human carcinoma cells. J Biol Chem *279*: 45495-45502, 2004.
22 Separovic D, Mann KJ and Oleinick NL: Association of ceramide accumulation with photodynamic treatment-induced cell death. Photochem Photobiol *68*: 101-109, 1998.
23 Boppana NB, Stochaj U, Kodiha M, Bielawska A, Bielawski J, Pierce JS, Korbelik M and Separovic D: C6-pyridinium ceramide sensitizes SCC17B human head and neck squamous cell carcinoma cells to photodynamic therapy. J Photochem Photobiol B *143*: 163-168, 2015.
24 Dolgachev V, Farooqui MS, Kulaeva OI, Tainsky MA, Nagy B, Hanada K and Separovic D: De novo ceramide accumulation due to inhibition of its conversion to complex sphingolipids in apoptotic photosensitized cells. J Biol Chem *279*: 23238-23249, 2004.
25 Hammad SM, Pierce JS, Soodavar F, Smith KJ, Al Gadban MM, Rembiesa B, Klein RL, Hannun YA, Bielawski J and Bielawska A: Blood sphingolipidomics in healthy humans: impact of sample collection methodology. J Lipid Res *51*: 3074-3087, 2010.
26 Luo J, Li L, Zhang Y, Spitz DR, Buettner GR, Oberley LW and Domann FE: Inactivation of primary antioxidant enzymes in mouse keratinocytes by photodynamically generated singlet oxygen. Antioxid Redox Signal *8*: 1307-1314, 2006.
27 Garcia-Calvo M, Peterson EP, Leiting B, Ruel R, Nicholson DW and Thornberry NA: Inhibition of human caspases by peptide-based and macromolecular inhibitors. J Biol Chem *273*: 32608-32613, 1998.
28 Oslowski CM and Urano F: Measuring ER stress and the unfolded protein response using mammalian tissue culture system. Methods Enzymol *490*: 71-92, 2011.
29 Cross BC, Bond PJ, Sadowski PG, Jha BK, Zak J, Goodman JM, Silverman RH, Neubert TA, Baxendale IR, Ron D and Harding HP: The molecular basis for selective inhibition of unconventional mRNA splicing by an IRE1-binding small molecule. Proc Natl Acad Sci USA *109*: E869-878, 2012.
30 Boyce M, Bryant KF, Jousse C, Long K, Harding HP, Scheuner D, Kaufman RJ, Ma D, Coen DM, Ron D and Yuan J: A selective inhibitor of eIF2alpha dephosphorylation protects cells from ER stress. Science *307*: 935-939, 2005.
31 Carlisle RE, Brimble E, Werner KE, Cruz GL, Ask K, Ingram AJ and Dickhout JG: 4-Phenylbutyrate inhibits tunicamycin-induced acute kidney injury *via* CHOP/GADD153 repression. PLoS One *9*: e84663, 2014.

Received December 15, 2016
Revised January 10, 2017
Accepted January 12, 2017